TISSUE ENGINEERING: Part C
Volume 15, Number 2, 2009

DOI: 10.1089/ten.tec.2008.0347

High-Throughput Measurements of Hydrogel Tissue Construct Mechanics

Juan Pablo Marquez, Ph.D.,[1,*] Wesley Legant, B.S.,[2,*] Vy Lam, Ph.D.,[1] Amy Cayemberg, B.S., MPT,[1] Elliot Elson, Ph.D.,[2,3] and Tetsuro Wakatsuki, Ph.D.[1,2]

Engineered tissues represent a natural environment for studying cell physiology, mechanics, and function. Cellular interactions with the extracellular matrix proteins are important determinants of cell physiology and tissue mechanics. Dysregulation of these parameters can result in diseases such as cardiac fibrosis and atherosclerosis. In this report we present a novel system to produce hydrogel tissue constructs (HTCs) and to characterize their mechanical properties. HTCs are grown in custom chambers and a robotic system is used to indent them and measure the resulting forces. Force measurements are then used to estimate HTC pretension (cellular contractility). Pretension was reduced in a dose-dependent manner by cytochalasin D (CD) treatment; the highest concentration (2 μM) resulted in ~10-fold decrease. On the other hand, treatment with fetal bovine serum (20%) resulted in approximately threefold increase in pretension. Excellent repeatability and precision were observed in measurements from replicate HTCs. The coefficient of statistical variance of quantified pretension ranged from 7% to 15% ($n = 4$). Due to the small size ($4 \times 4 \times 0.8$ mm) of the HTCs, this system of profiling HTC mechanics can readily be used in high-throughput applications. In particular, it can be used for screening chemical libraries in search of drugs that can alter tissue mechanics.

Introduction

Tissue engineering is rapidly becoming a critical area in scientific and clinical research and technology development. At the inception of the field, the primary focus was the development of functional substitutes for damaged tissues.[1] However, since then tissue engineering has become the foundation for developing novel tools for biomedical research.[2,3] To further increase the utility of this technology, we have developed a high-throughput (HTP) method of producing miniature hydrogel tissue constructs (HTCs) and an automated robotic system to quantify their physical properties—that is, tissue contractility and stiffness. Technologies to measure and analyze HTC physical properties, including contractility, have been introduced by other groups.[4–9] However, to the best of our knowledge, this is the first attempt at HTP application of HTC technology.

In contrast to traditional tissue culture systems where cells are grown on two-dimensional (2D) solid surfaces, HTCs consist of cells embedded in a three-dimensional (3D) hydrogel scaffold. Because this 3D scaffold provides a structural environment that more closely resembles *in vivo* conditions, cells grown in HTCs are arguably more natural physiologically than those cultured on 2D surfaces.[10] Further, 3D tissue constructs enable the quantification of physical and functional properties of extracellular matrix (ECM) components and the mechanical properties of the tissue as a whole. Alterations in cell physiology or cell–ECM interaction, such as increased cellular production of matrix proteins, can be quantified as changes in HTC mechanical properties. *In vivo*, altered tissue and organ mechanical homeostasis is known to be pathogenic and can result in diseases. An example is the contribution of scar tissue formation to the progression of cardiovascular diseases, e.g. cardiac fibrosis[11–13] and atherosclerosis. In cardiac fibrosis scar tissue formation and expansion impairs cardiac function by elevating tissue stiffness, and preventing cardiac relaxation, eventually leading to heart failure. In atherosclerosis the formation of scar-like tissue, which involves changes in smooth muscle cells from contractile to synthetic, results in impaired blood flow.[14,15] In both cases, tissue mechanics are altered when quiescent fibroblasts are transformed into myofibroblasts that contract the tissue and increase tissue stiffness by depositing excess ECM proteins. Improved understanding of the mechanisms by which these fibroblasts alter tissue integrity will facilitate the development

[1]Department of Physiology, and Biotechnology and Bioengineering Center, Medical College of Wisconsin, Milwaukee, Wisconsin.
[2]InvivoSciences LLC, McFarland, Wisconsin.
[3]Department of Biochemistry and Molecular Biophysics, Washington University School of Medicine, St. Louis, Missouri.
*These authors contributed equally to this work.

of drugs and therapies to prevent and possibly reverse disease progression.

In this report we present a method to produce miniaturized HTCs and an automated robotic system to quantify cellular contractility and HTC stiffness. The HTCs are approximately 4×4×0.8 mm in dimension and are compatible for HTP (96-well plate) assays, experiments, and screening procedures. A simple analysis to estimate active cellular and passive ECM mechanical properties was derived, and the results are compared to previous reports detailing how changes in HTC force generation can be decomposed into contributions from active cellular contraction and passive extracellular mechanical properties.[8,16] Reproducibility and repeatability of HTC force measurements were investigated. As a preliminary test for chemicals that altered cellular contractility and tissue mechanical properties, HTC forces were measured after cytochalasin D (CD) and fetal bovine serum (FBS) treatments. These results were compared to previous reports.[16] We propose that this HTC testing system can be used as an HTP screening system to find compounds that can alter tissue mechanics, and that this technology will greatly facilitate the discovery of pharmaceuticals to treat tissue-integrity dysfunction diseases such as fibrosis and atherosclerosis.

Materials and Methods

Cell and tissue culture

HTCs were generated by mixing cells and neutralized collagen as previously described.[8] Briefly, cells were mixed with neutralized rat-tail collagen (Millipore, Billerica, MA) and Dulbecco's modified Eagle's medium (DMEM; Sigma, St. Louis, MO) containing 10% FBS. A small amount (250 μL) of this solution was poured into each well of an eight-well polycarbonate mold (Fig. 1) and incubated at 37°C for 30 min to allow the collagen (1 mg in 1 mL gel solution) to polymerize and trap the cells within the collagen matrix. The tissues were then cultured in DMEM supplemented with 10% FBS and antibiotics (penicillin and streptomycin; Sigma) at 37°C for 2–3 days. During this time, the entrapped cells (1 million cells/1 mL gel solution) remodel and compact the tissue[17] by cell traction force. Final concentrations of cells and collagen in the remodeled samples are ~18 million/mL and ~18 mg/mL, respectively. For mechanical measurements, culture medium was switched to a HEPES-buffered DMEM, pH 7.4, maintained at 37°C in atmosphere.

Cells used in this study include (1) rat embryo fibroblasts (REF-52) (kind gift from Dr. Wysolmerski, Department of Neurobiology and Anatomy, West Virginia University School of Medicine) and (2) chicken embryo fibroblasts (CEFs). REF-52 cells were maintained in DMEM supplemented with 10% FBS and were passaged three times a week. CEFs were isolated from 10-day-old chicken embryos using a previously described method (8), and maintained in DMEM supplemented with 3% FBS. CEFs were used between 2 and 5 passages. All HTCs were prepared identically and tested following a 2–3 day incubation. Therefore, the size of each HTC including its cross-sectional area was almost identical.

Chemicals

To enhance or inhibit cell-force generation in HTCs, FBS or CD were added at least 30 min before mechanical testing. To reach the concentration of CD specified in the Results section, appropriate amounts of a stock solution (4 mM in dimethyl sulfoxide) were added to the media in which the HTCs were incubated. FBS was used undiluted. All materials were purchased from Sigma Chemicals (St. Louis, MO) unless otherwise specified.

Tissue chambers

A tabletop CNC mill (Sherline Products, Vista, CA) was used to machine 8 HTC cultivation chambers in individual

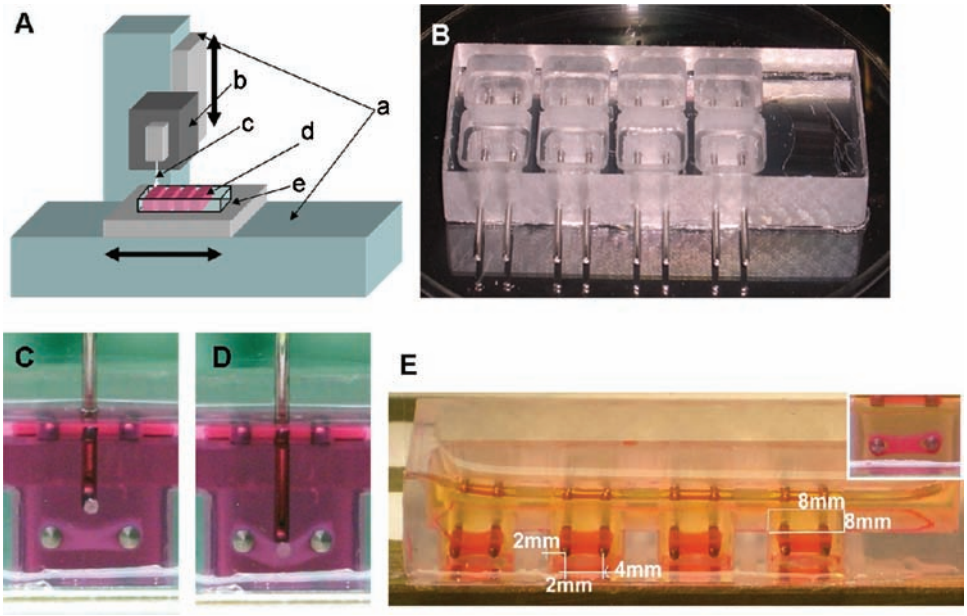

FIG. 1. (**A**) Schematic of the force measurement device. a, Linear actuator moved by a servo motor (±70 μm accuracy); b, isometric force transducer; c, force probe; d, tissue chamber; e, warming plate (37°C) connected to a water circulation bath. The device can automatically indent four samples in one row, and the operator manually translates the mold to the next row. A computer records the force response measured by the isometric transducer and regulates the speed of indentation. (**B**) Tissue chamber for producing and testing engineered tissues. (**C**) A force probe approaching an HTC formed between two stainless steel bars. (**D**) The probe indents the HTC vertically and stretches it longitudinally. (**E**) The typical size of HTCs was approximately 4×4×0.8 mm (length×width×thickness), and they are formed in 8×8 mm (opening) square wells in the tissue chamber. Color images available online at www.liebertonline.com/ten.

polycarbonate blocks (25×60×10 mm). The eight square wells of 8×8 mm were each embedded with two horizontal medical grade stainless-steel bars (1 mm diameter) that were located 2 mm above the bottom of the well and 2 mm from the side walls. The bars were spaced 4 mm apart (Fig. 1A). The bottom of the wells (Fig. 1B) was closed with a microscope coverslip (No. 1 thickness, Fisher, Pittsburgh, PA) and sealed using silicon glue (Dow Chemicals, Midland, MI). A coverslip was used to facilitate further microscopic imaging of the cells and HTCs. The chambers were sterilized by ethylene oxide gas treatment at the VA Medical Center (Milwaukee, WI), and kept in 100 mm sterile Petri dishes to prevent contamination. The cell–matrix solution was poured into the wells and immersed the horizontal bars. During tissue culture, HTCs detach from the bottom and side walls, stiffen to form a compact membrane of tissue that stretched between the bars, and produce an active tension.

Testing device

The mechanical testing device was developed by InvivoSciences LLC (McFarland, WI). A horizontal linear actuator (Fig. 1A-a; ER32-SRN300A; Parker, Wadsworth, OH) automatically placed the center of each well directly below an L-shaped force probe (0.8 mm diameter, Fig. 1C), which indented the middle of the HTC and stretched it longitudinally (Fig. 1D). The other end of the probe was connected to an isometric force transducer (Fig. 1A-b; 0.5 g/5.0 range, 1/1000 sensitivity; Harvard Apparatus, South Natick, MA), which was moved by a vertical linear actuator (Fig. 1A-a; ER32-SRN100A; Parker). The accuracy of positioning the probe and indenting the tissue is determined by accuracy (±70 μm) of the linear actuators. Background noise level of force detection was less than 0.1 mN. During testing, the temperature of HTCs in the wells was kept at 37°C using a water-jacketed warm plate (Fig. 1A-e) connected to a circulating water bath (HAAKE C10-P5; Thermo Fisher Scientific, Waltham, MA). The linear actuators were controlled simultaneously by a personal computer that also recorded the signal from the force transducer. Time-dependent extension and withdrawal of the force probe was programmed using computer software that controls the actuators' displacement. The molds containing the HTCs could be quickly positioned for mechanical measurement by sitting them in a placeholder. The force measurement device was placed in a laminar flow hood to prevent contamination of the HTCs during testing. Maintenance of sterility allowed for continued mechanical measurement of the same HTCs over the course of hours, days, or weeks.

Data analysis

We modified a simple linear mechanical model to analyze mechanical properties of HTCs. Development and various assumptions of the model are described in the Results section. All of the analysis software was written using MATLAB® (Mathworks, Natick, MA).

Theoretical analysis of membrane deformation and force generation

We have developed a simple method of analyzing force data recorded from the vertical stretching of an HTC membrane. As the probe pushes down on the HTC at a constant rate, v (0.5 mm/s), an isometric force transducer connected to the probe records the resistance force, $F(t)$, generated by HTC-membrane deformation (Fig. 1). At any given time, t, the HTC is vertically indented a distance $d(t)$, $(=vt)$, by the L-shaped probe. As a result, the HTC is stretched longitudinally, $\Delta L(t)$, from its initial length, L_0 (Fig. 2). Using trigonometric relationships, a longitudinal force representative of HTC tension, $T(t)$, is calculated as

$$T(t) = \frac{F(t)}{2\sin\alpha(t)} \tag{1}$$

where $\alpha(t)$ is the small angle between the HTC membrane and the horizontal plane.

To characterize the material properties of HTCs, tissue strain, $\varepsilon(t)$, and stress, $\sigma(t)$, are defined in terms of $\Delta L(t)$, $F(t)$, L_0, and the cross-sectional area of the HTC, A. The strain is expressed as a function of $d(t)$ by

$$\varepsilon(t) = \frac{\Delta L(t)}{L_0} = \frac{1}{L_0}\left(\sqrt{L_0^2 + [2d(t)]^2} - L_0\right) = \sqrt{1 + \left(\frac{2d(t)}{L_0}\right)^2} - 1. \tag{2}$$

The stress is also expressed as a function of $d(t)$ and $F(t)$ by

$$\sigma(t) = \frac{T(t)}{A} = \frac{F(t)}{2A\sin\alpha(t)} = \frac{F(t)\sqrt{1 + \left(\frac{2d(t)}{L_0}\right)^2}}{2A\frac{2d(t)}{L_0}}. \tag{3}$$

A typical experimental plot of $F(t)$ versus $[d(t)/L_0]$ is shown in Figure 3A. The data were transformed into a plot of $T(t)$ versus $\varepsilon(t)$ in Figure 3B using Equations 2 and 3. At low strain $[\varepsilon(t) < 1.5\%]$, tissue tension, $T(t)$, was artificially increased as Equation 2 approached 0 at $d(t) = 0$. On the other hand, at high strain $[\varepsilon(t) > 10\%]$, tissue tension increased nonlinearly (Fig. 3B). In the intermediate range of 1.5% to 7%, the tissue tension increased linearly with strain and behaved

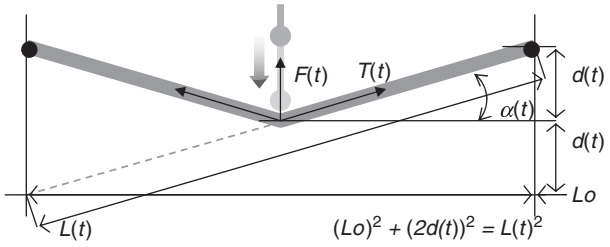

FIG. 2. Theoretical trigonometric relationship of HTC indentation and stretching. An HTC of negligible thickness and length L_0 (before the indentation, $t = 0$) is represented by the thick solid line attached to two horizontal bars (black dots). The force probe (dot with line) pushes the HTC vertically, $d(t)$, at its center. As the probe advances, the force $F(t)$ recorded by the transducer and the longitudinal force, $T(t)$, increase because of HTC resistance to the deformation. The trigonometric relationship of longitudinal force developed in the HTC, $[F(t) = 2T(t)\sin\alpha]$, vertical indentation depth, $d(t)$, HTC length at time t, $L(t)$, and 0, L_0, is illustrated by the dotted line.

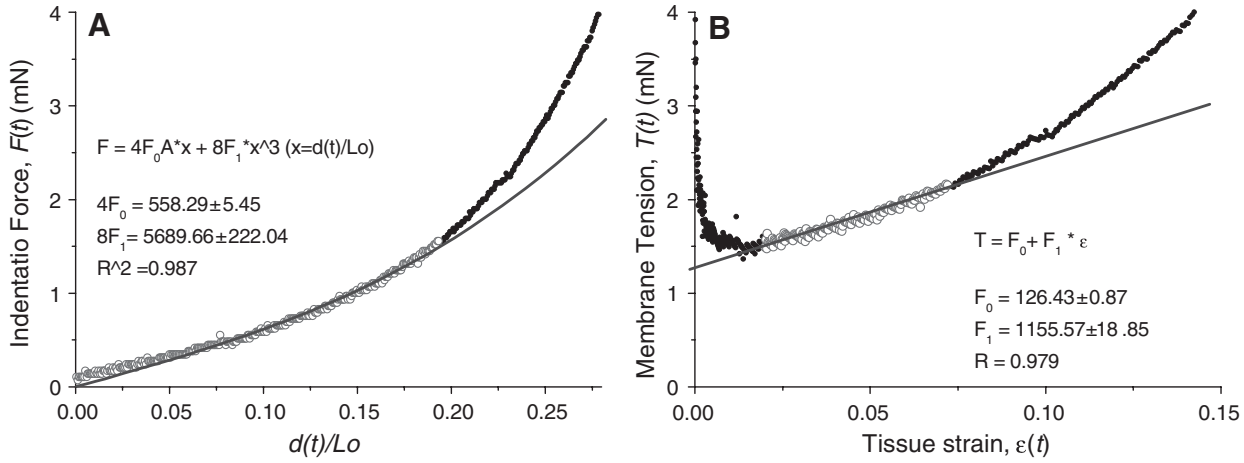

FIG. 3. Estimating HTC pretension and elastic force. (**A**) Force response, $F(t)$, is plotted against $\Delta Z(t)$, that is, $[d(t)/L_0]$. Data points before the probe touch the sample are not shown. An example of polynomial curve fitting to estimate F_0 and F_1 is shown as a solid line. Only data points indicated by the red open circles, indentation $< 7\%$ strain, are used for curve fitting. (**B**) Force response versus $d(t)/L_0$ plots are converted to longitudinal force, $T(t)$, versus strain plots. Because the conversion of F to T introduced a singularity at zero strain, T increases as strain approaches zero. Linear regression of the data points in the middle portion, $0.02 < \varepsilon < 0.07$ (red circles), is used to estimate F_0 and F_1. Color images available online at www.liebertonline.com/ten.

similar to an isotropic linear elastic material with modulus of elasticity, E. This behavior can be expressed as:

$$\sigma(t) = E\varepsilon(t) + \sigma_0, \tag{4}$$

where σ_0 is the prestress of the HTC membrane.

Even though HTCs are a highly nonlinear mechanical material, we used this simplified equation as an initial model of their mechanical behavior. Because HTCs are very soft and their edges are connected to thin bars, bending and shear force were assumed to be negligible. This model allows us to estimate tissue prestress and the modulus of elasticity through data fitting. When Equation 4 is multiplied by the cross-sectional area of the HTC, A, we obtain:

$$T(t) = A\sigma(t) = EA\varepsilon(t) + \sigma_0 A = F_1(t) + F_0, \tag{5}$$

where F_1 and F_0 are defined as elastic force and pretension (unit of force), respectively.

This tissue tension equation was used to fit the force measurements from tissue strain ranging from 1.5% to 7% strain. Linear regression of the data yielded a slope indicating the elastic force of the tissue, F_1, and an intercept that corresponded to the tissue pretension, F_0 (Fig. 3B). This pretension in the tissue was generated by cellular remodeling of the collagen matrix (over several hours to days), by cellular traction, as well as by acute cellular contractile force in response to various activators.

Analysis of the tension, $T(t)$, data were limited due to the singularity introduced by the conversion of $F(t)$ to $T(t)$. To avoid this limitation, an alternative analytical equation for the indentation force, $F(t)$, was derived. For small indentation distances, where $2d(t)/L_0 < 0.5$, strain and stress in Equations 2 and 3 can be approximated as:

$$\varepsilon(t) \approx \frac{1}{2}\left(\frac{2d(t)}{L_0}\right)^2 = 2[\Delta Z(t)]^2, \tag{6}$$

and

$$\sigma(t) \approx \frac{F(t)}{2A\left(\frac{2d(t)}{L_0}\right)} = \frac{F(t)}{4A\Delta Z(t)}, \tag{7}$$

where $\Delta Z(t) = d(t)/L_0$. By combining Equation 4 with Equations 6 and 7, while satisfying $2d(t)/L_0 < 0.5$, we can rewrite the measured indentation force as a simple cubic polynomial function of $\Delta Z(t)$:

$$F(t) = 4F_0\Delta Z(t) + 8F_1[\Delta Z(t)]^3, \tag{8}$$

The slope, $dF(t)/d(\Delta Z(t))$, of the curve is expected to change when the probe touches the tissue surface at $t = \tau$. Because Equation 8 represents $F(t)$ only after the tissue is indented, a more general expression is used to estimate F_1, F_0, and the time offset, τ (Fig. 3A):

$$F(t) = 4F_0\Delta Z(t-\tau) + 8F_1[\Delta Z(t-\tau)]^3; \quad t \geq \tau \text{ and } F(t) = 0 \text{ for } t < \tau. \tag{9}$$

The value of F_0 estimated by the linear and cubic polynomial functions was relatively close, 126.43 ($\pm$0.87) mN and 139.57 ($\pm$1.36) mN, respectively (Fig. 3B and A). In further analyses τ was estimated by curve fitting of Equation 9 to the data.

Results

Repeatability and reproducibility of HTC mechanical measurements

Repeatability of HTC mechanical measurement was analyzed by a series of stretches. All HTCs used in the analysis were kept in DMEM containing 10% FBS for 2 days after their production, and then switched to serum-free DMEM 16 h before testing. Each HTC was vertically indented eight

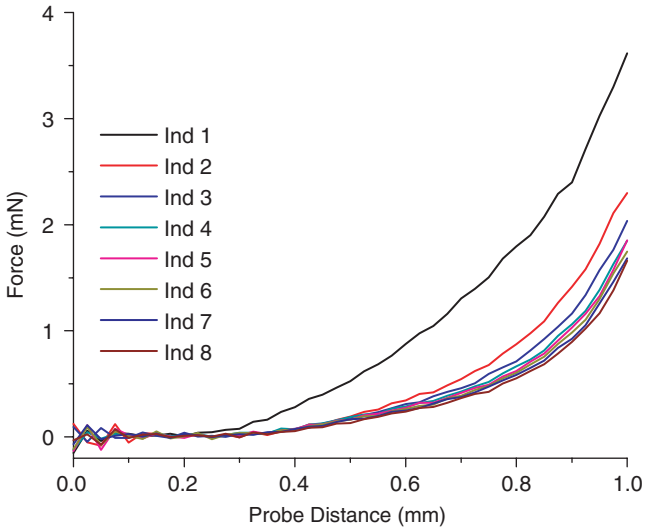

FIG. 4. Effect of the number of indentations on HTC mechanics. An HTC membrane constructed of REFs was stretched eight times at 5 min intervals. Initial force responses were higher than subsequent ones, but this decrease in force became negligible after three indentations. Color images available online at www.liebertonline.com/ten.

times, each with a resulting 20% longitudinal stretch. The recorded force–response curve gradually decreased until the third or fourth indentation, after which the measurements converged and further reductions were negligible (Fig. 4). This convergence of tissue properties after repeated stretching is a known preconditioning effect that is observed in biomechanical investigations of animal tissues.[18,19] Due to this preconditioning effect, all experiments and data presented in the following sections were preceded by three or more preconditioning indentations.

The repeatability of mechanical measurements is crucial for comparing experimental results and adapting the assay for HTP applications. After three preconditioning stretches, typical force–time curves obtained from four replicate HTCs showed similar response profiles (Fig. 5A). However, an offset was observed where the force profile increased above background (inset, Fig. 5A). This artifact was due to the HTCs forming at different heights and thus the probe contacted each one at a slightly different time. If the force curves were time-shifted to synchronize contact time, the measured forces overlapped and became indistinguishable from each other (Fig. 5B). This result demonstrates that mechanical measurements of the HTCs are highly repeatable.

The reproducibility of HTC mechanical measurements was also investigated. HTCs prepared on different days were treated with the same concentrations of CD, which reduced HTC forces (See Quantification of HTC pretension in response to chemical treatment). The data yielded comparable dose-dependent curves for CD effects on cell contractility (Supplemental Fig. S1, available online at www.liebertonline.com/ten). This result suggests that the HTCs behave similarly from batch to batch and that the quantified tissue mechanics are stable.

To investigate the limitations of instrumentation, the stability of force measurements was monitored relative to the rate of data acquisition and indentation speed. To maximize the throughput of experiments, it is desirable to minimize the force measurement time. However, increased rates of probe movement, which increase the rate of HTC deformation and data acquisition, may cause mechanical vibrations that generate noise in the force measurements. Varying

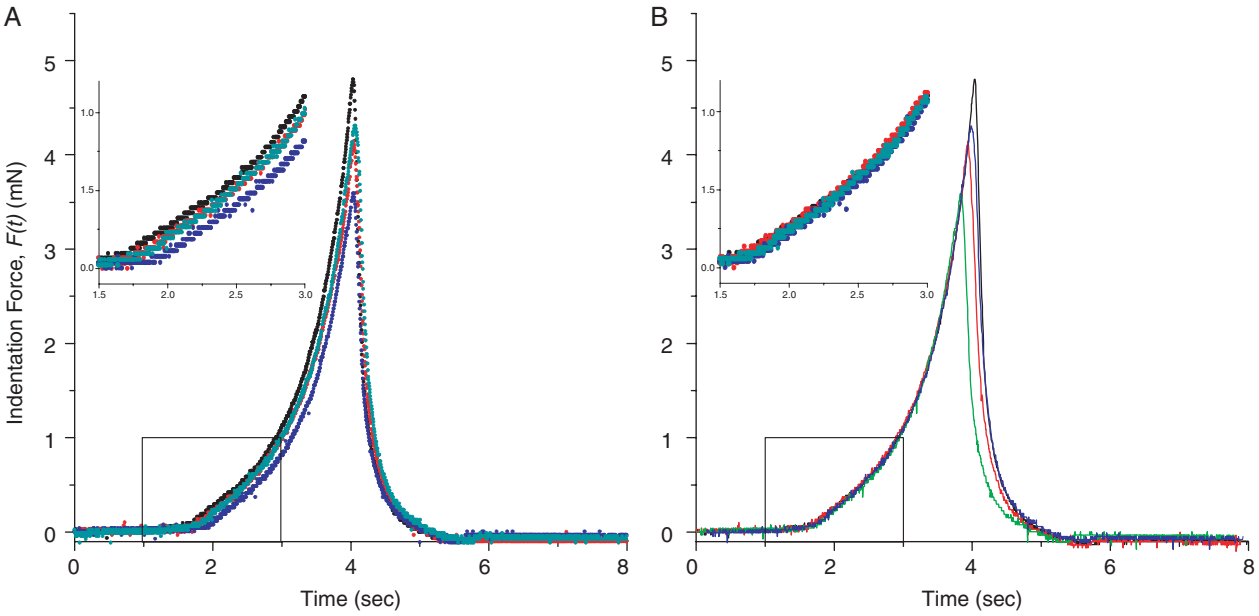

FIG. 5. (**A**) Representative force measurements from four HTCs. (**B**) The curves overlap when each data set is adjusted with a time-delay offset to synchronize the time when the probe touches the HTCs. Insets (regions in square were zoomed in) show graph details at the transition points where force measurements deviate from zero. Color images available online at www.liebertonline.com/ten.

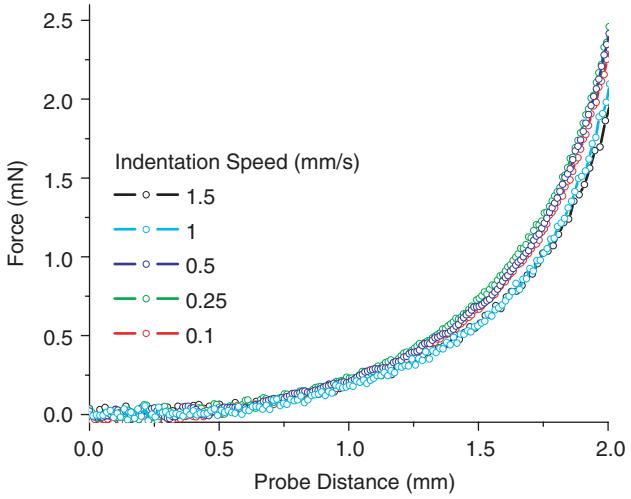

FIG. 6. Effect of indentation speed on force–response curves. Increasing vertical indentation speed from 0.1 to 1.5 mm/s produced a minimal increase in the noise level of force recordings. There was no significant difference in slopes at all speeds tested. Color images available online at www.liebertonline.com/ten.

indentation speeds between 0.1 and 1.5 mm/s showed nominal variation in force measurements, $F(t)$ (Fig. 6). This independence of measured force relative to the rate of HTC deformation suggests that instrument stability is not a factor, which is in agreement with previously reported results.[19] Although the quality of data acquisition was equivalent at all tested indentation rates, 0.5 mm/s was used in all subsequent experiments.

Quantification of HTC pretension in response to chemical treatments

To demonstrate an application of this force measurement and data analysis system, CD treatments were used to reduce HTC pretension. Because CD disrupts the actin cytoskeleton of cells and thus prevents the transmission of contractile forces to the ECM, increasing doses of CD should reduce the resistance force to stretching and shift the $F(t)$ profile downward. Results showed that CD treatment did indeed reduce the pretension in the HTCs (Fig. 7A). Further, HTCs treated with the highest concentrations of CD produced little force, and their $F(t)$ curves showed a smooth transition between background and stretched forces. Accurate estimation of τ at these higher CD concentrations was difficult due to the smooth transition of the $F(t)$ curves that obscured the time of initial contact between the probe and the HTCs. The downward shift of the data was also apparent in the $T(t)$ curves (Fig. 7B). The F_0 and F_1 of these data curves were estimated using both linear regression and cubic polynomial fitting. The two models produced similar results with F_0 decreasing as CD concentration increased (Fig. 8A). However, the F_1 values from the linear model were slightly higher than the values from the cubic model (Fig. 8B). This was particularly evident at lower concentrations of CD.

Previous studies have shown that tissue constructs contract acutely in response to treatment with 20% (v/v) FBS in medium.[8] As a positive control, four HTCs were treated with 20% FBS immediately after the third preconditioning indentation (Fig. 9A). The same HTCs were indented every 5 min for 30 min after FBS treatment. Additional HTCs were treated with CD (2 μM), while others were indented in clean culture media for use as nontreated controls. The F_0 of the HTCs demonstrated an acute threefold increase and twofold decrease of HTC pretension in response to FBS and CD treatments, respectively. This observed result is in agreement with those previously reported.[8] After the initial preconditioning indentations, the estimated F_0 of the control group did not change over the test period. Further, in agreement with results shown in Figure 3, box plots of control, FBS, and CD-treated groups in this experiment showed high repeatability of the data (Fig. 9B).

Quantitative comparison to other tissue constructs: effects of CD on cellular mechanics

Tissue pretension data from our miniature HTC testing system were compared with that obtained from a previously

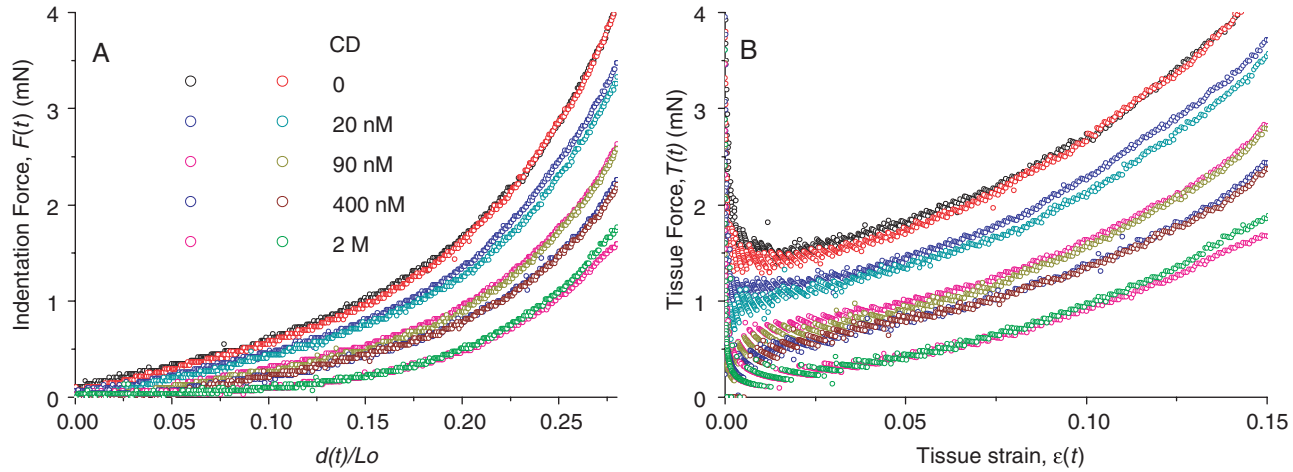

FIG. 7. (**A**) Duplicate HTCs were treated with 0, 20, 90, 400, or 2000 nM CD. Increasing the concentration of CD reduced the resistant force, $F(t)$, in a dose-dependent manner. (**B**) CD treatments shifted the $T(t)$ versus strain plots down, but their initial slope is maintained. Color images available online at www.liebertonline.com/ten.

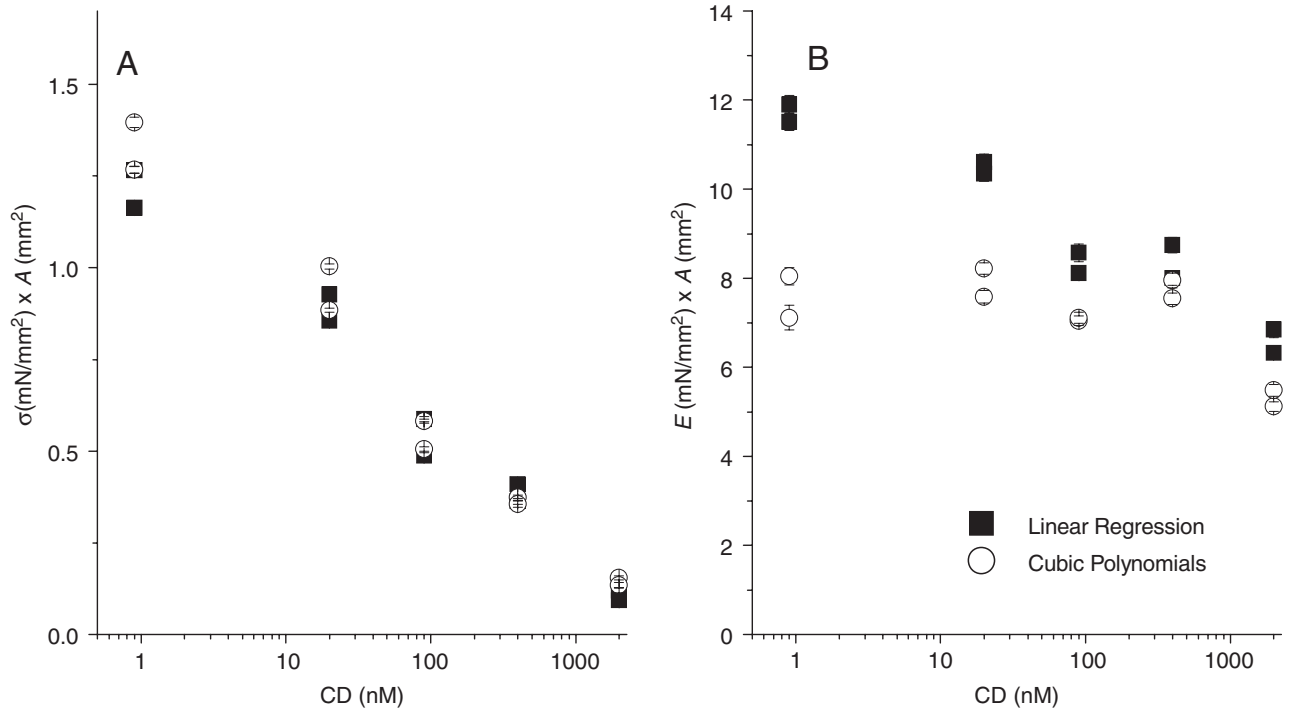

FIG. 8. (**A**) The concentration-dependent reduction in pretension, F_0, was nearly identical whether estimated via linear regression or cubic polynomial fitting. (**B**) The elastic force of the HTCs, F_1, estimated via the two methods did not overlap, especially when obtained from HTCs treated with lower concentrations of CD. The values of F_1 estimated via the cubic polynomial method were relatively unchanged until the highest concentrations of CD.

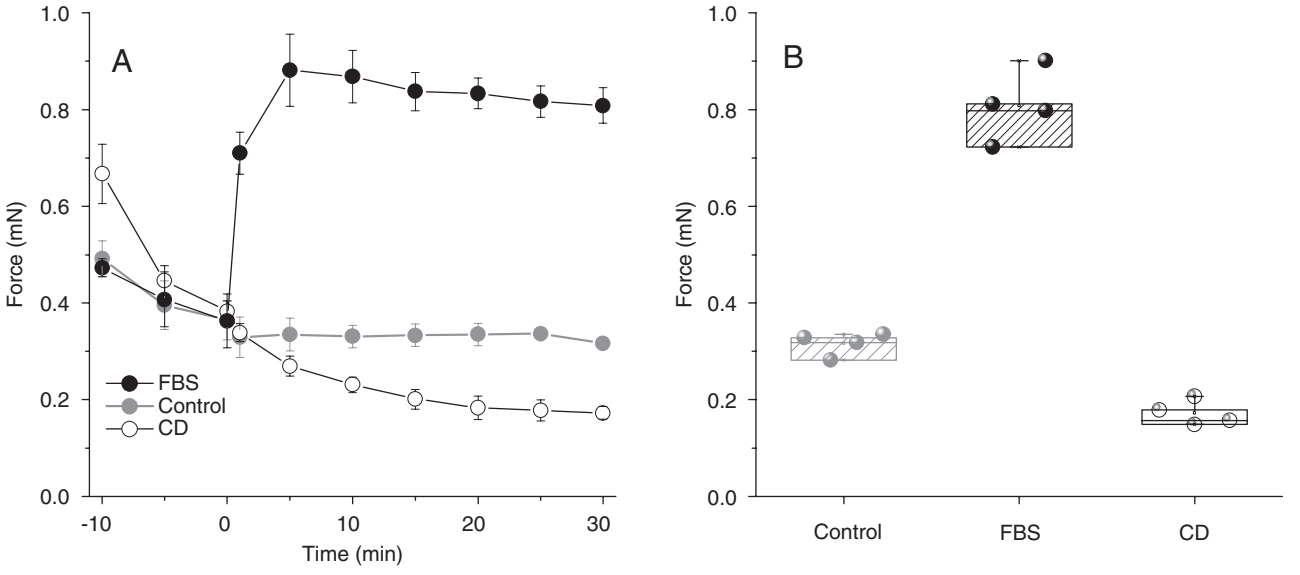

FIG. 9. (**A**) Time-dependent changes in pretension, F_0, in contracting and relaxing HTCs. Immediately after the third preconditioning indentation, one group of HTCs was treated with 20% FBS, another group was treated with 2 μM CD, and a third untreated group served as the control. The untreated control group showed almost no change in force after the preconditioning indentations. However, forces in the FBS-treated group showed a rapid increase, and those in the CD-treated group showed a slow decrease. (**B**) Box plots of representative control, FBS, and CD treated force data at 30 min post-treatment showing high data reproducibility between replicate samples ($n = 4$). Differences in the control versus FBS, control versus CD, and FBS versus CD data are statistically significantly ($p < 0.05$).

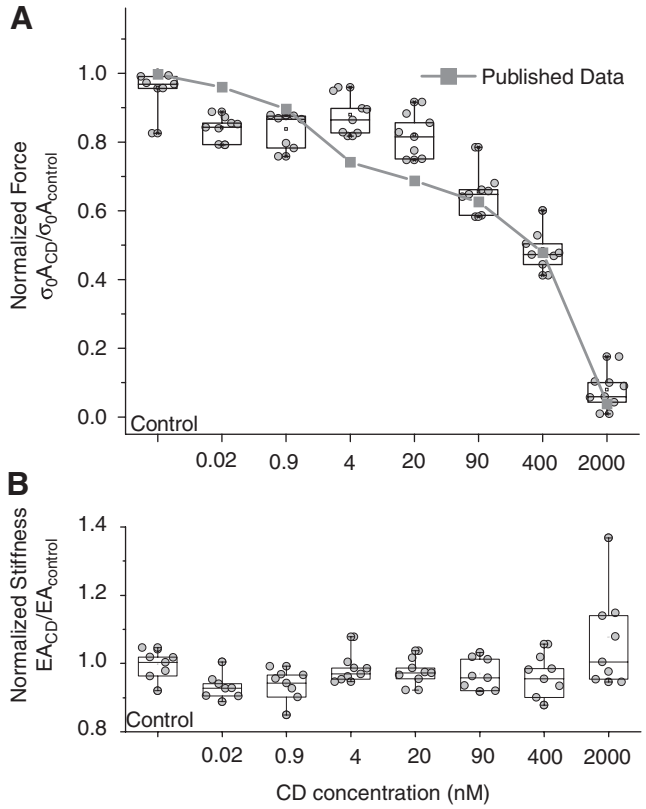

FIG. 10. (**A**) Box plots illustrating the effects of CD treatment on CEF tissues. Ratio of active cell force after CD treatment to before treatment was plotted for the eight different CD concentrations. Eight HTC samples were measured at each concentration (red plus indicate outlier). Squares connected by a dotted line represent data from ring-shaped tissues as previously reported.[16] (**B**) No changes were observed in tissue elastic force, F_1, (defined in Eq. 5) after CD treatment.

published report using the ring-tissue system.[16] In the previous study, the effect of CD on the mechanical properties of ring-shaped CEF tissue constructs (CEF-rings) was analyzed using a force measurement apparatus similar to those used for aortic ring research.[20] The apparatus consisted of a force transducer connected to a vertically suspended hook holding the top of the tissue ring and a stationary hook attached to the bottom. In this ring-stretching system, the direction of contractile force was parallel to the direction of stretch. This is in contrast to our current system where HTC contractile force is developed perpendicular to the direction of stretch.

To be consistent with the previous study, CEFs were used to construct miniature CEF-HTCs. After three preconditioning stretches, different concentrations of CD were added (200 pM, 900 nM, 4 nM, 20 nM, 90 nM, 400 nM, and 2 μM) to 4–6 CEF-HTCs. Forty-five minutes after the addition of CD, pretension was measured by additional stretches. The quantified pretension was normalized to the pretension from before CD treatment and plotted (Fig. 10). The dose-dependent decrease in CEF-HTC pretension in response to CD treatment was almost identical to that previously observed[16] (Fig. 10, squares with solid line). This result demonstrates that our miniature HTCs, along with our data analysis system, can effectively reproduce previously observed phenotypes and can thus be used for continued investigation of cellular behavior and tissue mechanics.

Discussion

Data analysis and mathematical modeling of tissue mechanics

In this report, we presented and tested a method to produce miniature HTCs and an automated robotic system to record HTC mechanical forces. A cubic function was used to model the HTC force data and estimate the pretension and elastic force of the HTCs. This analysis allowed us to quantify the mechanical properties of a large number of tissues and evaluate their responses to environmental challenges. HTC pretension appears to be a more robust indicator of HTC mechanics than HTC elastic force. HTC pretension quantitatively reflected the contractility reducing activity of CD and the inducing effect of FBS.

The larger variance in HTC elastic force may be due, in part, to the limitations and assumptions inherent in the fitting models (Fig. 8). First, different numbers of data points are fitted. The linear regression method was applicable for data points between 1.5% and 7% tissue strain, whereas the polynomial fitting method incorporated data below 1.5%. Second, the models assume that the HTC is a band of uniform thickness and width with a uniform stress–strain distribution. Because HTCs are very soft and held by small diameter pins, the bending and shear forces were neglected. Although there are some limitations to the application of Saint-Venant's principle, it is reasonable to assume a homogeneous stress–strain distribution along the HTC, but not at the edges where it attaches to the bars. Third, neither model currently accounts for nonlinearity in HTC behavior. Mechanical properties of biological tissues, including HTCs, are known to be nonlinear, particularly at high strain levels.[8,18] Currently, parameters estimated via cubic polynomial fitting are preferred for analyzing data because it allows for the direct estimation of τ, that is, when the probe touches the HTC's upper surface. We have manually confirmed the coincidence of the estimated τ and the actual time of probe–HTC contact using video recording of the probe indenting the HTC (Supplemental Movie 1 and Supplemental Fig. S2, available online at www.liebertonline.com/ten). To improve the analysis of HTC elastic force, we plan to develop a more sophisticated data analysis methodology that will enable us to better describe the nonlinear nature of HTC mechanics and alterations in HTC shape as it is deformed. Nevertheless, the presented method provides sufficient information about the biomechanical parameters of tissue constructs in high throughput. The accurate assessment of HTC stress and modulus of elasticity requires different approaches that have been previously developed.[8]

Repeatability and precision of engineered tissue constructs

As one would expect, the major sources of systematic error in the data are from (1) improper preparation of HTCs and (2) measurement errors by the robotic system. It is critical to minimize these errors to maximize the repeatability (intra-batch) and reproducibility (inter-batch) of force measure-

ments. This is especially critical if HTCs are to be used for HTP applications. We find that the consistency of the HTCs depends on the continual mixing of the cell–matrix solution before it is dispensed into the wells. Cells suspended in the cell–matrix solution settle to the bottom relatively quickly so insufficient mixing of the solution during dispensing will result in larger pretension variance. To improve the pretension consistency of mass-produced HTCs, large volumes of the cell–matrix solution should be immediately divided into smaller aliquots so each can be mixed carefully before it is distributed into the wells.

Misalignment of the force measurement probe can also cause large variances in pretension measurement. Even though the robotic system is capable of positioning the probe precisely (±70 μm accuracy), initial deviation of the probe position from the center of the HTC will result in erroneous force measurements. The operator of the device is required to confirm probe alignment before each experiment. To facilitate this alignment process, a metal bracket was designed and attached to the warming plate to exactly position and align the eight-well chambered molds.

Another potential source of error would be irreversible damage of the HTCs due to excessive probe extension and HTC stretching. However, our testing showed that the range of HTC deformation used in our analyses was not detrimental to the tissues. Varying the probe movement distance from 1.6 to 2.0 mm (i.e., HTCs strain of 0.14 to 0.2) yielded comparable values of F_1, F_0, and τ (Supplemental Fig. S3, available online at www.liebertonline.com/ten). Even though all of the data presented in this report were from 2.0 mm stretches, shorter distances would have yielded comparable results.

Applications in drug discovery and disease investigation

In recent years there has been an enormous expansion of chemical libraries[21] available for discovering potential drugs. It is, however, a challenging task to efficiently screen these compounds for pharmaceutical utility and to do so at reasonable cost. Current HTP screening methods generally examine chemical interactions between candidate compounds and selected target molecules, such as protein kinases, *in vitro*. However, these methods rarely provide information about the biological activity or safety of the compounds. Typically, physiological and biological effects are not tested against cultured cells or animals until later stages of the drug discovery process.[22] To improve the productivity of HTP screening, platforms that can simultaneously measure intracellular and extracellular biological responses are critically needed. Toward this end, we are adapting our miniature HTCs, and the robotic system, for the quantification of cellular physiology and tissue mechanics in a 96-well plate format. We are also adapting existing fluorometric and colorimetric assays of cell physiology for use with the HTCs. Presented results from experiments with FBS and CD, which increase and decrease the force of tissue contraction, respectively, suggest that this HTC system can reliably quantify the dose-dependent and time-dependent changes in HTC mechanical properties in response to drug treatments. Further, these results suggest that the HTCs can be used for screening compound libraries in search of drug candidates that can mediate cellular contractility and tissue stiffness. Efforts are underway in our laboratory to produce HTC models of fibrosis and test for compounds that can arrest or reverse fibrotic progression.

We propose that this HTC production and mechanical testing system can be used to assess cellular and tissue responses to various types of biologically active agents, including chemical compounds, growth factors, DNAs, microRNAs (e.g., sh RNAs), viruses, and bacteria. The use of HTCs to model tissue mechanical properties and to quantify how altered cellular activity can change ECM composition and tissue function *in vitro* is a novel paradigm that cannot be achieved with traditional 2D cell cultures. Further miniaturization and automation of this system will facilitate its use in HTP pharmaceutical and toxicology screening. Because HTCs closely resemble natural tissue structure and physiological function, HTC-based assay systems will greatly facilitate *in vitro* cellular and tissue research and potentially become an alternative technology for animal studies.

Acknowledgments

The authors thank Maria Bravo and Dr. Matthew Peterson for all the insightful discussions and collaboration on this work. The work was supported partly by NIH Grants GM069072-01 and AT003984-01.

Disclosure Statement

No competing financial interests exist.

References

1. Langer, R., and Vacanti, J.P. Tissue engineering. Science **260,** 920–926, 1993.
2. MacNeil, S. Progress and opportunities for tissue-engineered skin. Nature **445,** 874–880, 2007.
3. Langer, R., and Tirrell, D.A. Designing materials for biology and medicine. Nature **428,** 487–492, 2004.
4. Tranquillo, R.T., Durrani, M.A., and Moon, A.G. Tissue engineering science: consequences of cell traction force. Cytotechnology **10,** 225–250, 1992.
5. Kolodney, M.S., and Wysolmerski, R.B. Isometric contraction by fibroblasts and endothelial cells in tissue culture: a quantitative study. J Cell Biol **117,** 73–82, 1992.
6. Tomasek, J.J., Haaksma, C.J., Eddy, R.J., and Vaughan, M.B. Fibroblast contraction occurs on release of tension in attached collagen lattices: dependency on an organized actin cytoskeleton and serum. Anat Rec **232,** 359–368, 1992.
7. Eastwood, M., McGrouther, D.A., and Brown, R.A. A culture force monitor for measurement of contraction forces generated in human dermal fibroblast cultures: evidence for cell-matrix mechanical signalling. Biochim Biophys Acta **1201,** 186–192, 1994.
8. Wakatsuki, T., Kolodney, M.S., Zahalak, G.I., and Elson, E.L. Cell mechanics studied by a reconstituted model tissue. Biophys J **79,** 2353–2368, 2000.
9. Bacia, K., Kim, S.A., and Schwille, P. Fluorescence cross-correlation spectroscopy in living cells. Nat Methods **3,** 83–89, 2006.
10. Zahir, N., and Weaver, V.M. Death in the third dimension: apoptosis regulation and tissue architecture. Curr Opin Genet Dev **14,** 71–80, 2004.
11. Frangogiannis, N.G., Smith, C.W., and Entman, M.L. The inflammatory response in myocardial infarction. Cardiovasc Res **53,** 31–47, 2002.

12. Frangogiannis, N.G., Michael, L.H., and Entman, M.L. Myofibroblasts in reperfused myocardial infarcts express the embryonic form of smooth muscle myosin heavy chain (SMemb). Cardiovasc Res **48,** 89–100, 2000.
13. Seidman, J.G., and Seidman, C. The genetic basis for cardiomyopathy: from mutation identification to mechanistic paradigms. Cell **104,** 557–567, 2001.
14. Dauerman, H.L. Treatment of stent restenosis: moving beyond momentum. J Am Coll Cardiol **47,** 2161–2163, 2006.
15. Serruys, P.W., Kutryk, M.J., and Ong, A.T. Coronary-artery stents. N Engl J Med **354,** 483–495, 2006.
16. Wakatsuki, T., Schwab, B., Thompson, N.C., and Elson, E.L. Effects of cytochalasin D and latrunculin B on mechanical properties of cells. J Cell Sci **114,** 1025–1036, 2001.
17. Tranquillo, R.T. Self-organization of tissue-equivalents: the nature and role of contact guidance. Biochem Soc Symp **65,** 27–42, 1999.
18. Fung, Y.C. Biomechanics. Mechanical Properties of Living Tissues, second edition. New York: Springer-Verlag, 1993.
19. Wagenseil, J.E., Elson, E.L., and Okamoto, R.J. Cell orientation influences the biaxial mechanical properties of fibroblast populated collagen vessels. Ann Biomed Eng **32,** 720–731, 2004.
20. Griffith, T.M., Henderson, A.H., Edwards, D.H., and Lewis, M.J. Isolated perfused rabbit coronary artery and aortic strip preparations: the role of endothelium-derived relaxant factor. J Physiol **351,** 13–24, 1984.
21. Ramstrom, O., and Lehn, J.M. Drug discovery by dynamic combinatorial libraries. Nat Rev Drug Discov **1,** 26–36, 2002.
22. Matsumoto-Ida, M., Akao, M., Takeda, T., Kato, M., and Kita, T. Real-time 2-photon imaging of mitochondrial function in perfused rat hearts subjected to ischemia/reperfusion. Circulation **114,** 1497–1503, 2006.

Address reprint requests to:
Tetsuro Wakatsuki, Ph.D.
Department of Physiology
Medical College of Wisconsin
8701 Watertown Plank Road
Milwaukee, WI 53226

E-mail: twakatsuki@mcw.edu

Received: June 20, 2008
Accepted: October 21, 2008
Online Publication Date: January 16, 2009